



LUND UNIVERSITY

Wireless Body Area Network for Heart Attack Detection

Wolgast, Georg; Ehrenborg, Casimir; Israelsson, Alexander; Helander, Jakob; Johansson, Edvard; Månefjord, Hampus

Published in:
IEEE Antennas and Propagation Magazine

DOI:
[10.1109/MAP.2016.2594004](https://doi.org/10.1109/MAP.2016.2594004)

2016

[Link to publication](#)

Citation for published version (APA):

Wolgast, G., Ehrenborg, C., Israelsson, A., Helander, J., Johansson, E., & Månefjord, H. (2016). Wireless Body Area Network for Heart Attack Detection. *IEEE Antennas and Propagation Magazine*, 58(5), 84-92. <https://doi.org/10.1109/MAP.2016.2594004>

Total number of authors:
6

Creative Commons License:
CC BY-NC-ND

General rights

Unless other specific re-use rights are stated the following general rights apply:
Copyright and moral rights for the publications made accessible in the public portal are retained by the authors and/or other copyright owners and it is a condition of accessing publications that users recognise and abide by the legal requirements associated with these rights.

- Users may download and print one copy of any publication from the public portal for the purpose of private study or research.
- You may not further distribute the material or use it for any profit-making activity or commercial gain
- You may freely distribute the URL identifying the publication in the public portal

Read more about Creative commons licenses: <https://creativecommons.org/licenses/>

Take down policy

If you believe that this document breaches copyright please contact us providing details, and we will remove access to the work immediately and investigate your claim.

LUND UNIVERSITY

PO Box 117
221 00 Lund
+46 46-222 00 00

IEEE AP-S Student Design Contest 2015

Team Gerhards Grabbar

Georg Wolgast, Casimir Ehrenborg, Alexander Israelsson, Edvard Johansson and Hampus Månefjord

Abstract—This paper describes a body area network for measuring an electrocardiogram signal and transmitting it to a smartphone via Bluetooth for data analysis. The body area network uses a specially designed planar inverted F-antenna whose design prioritizes size, cost and efficiency. Due to the human body's electrical properties, the antenna was designed to enable surface wave propagation around the body. The system utilizes the user's own smartphone for data processing, while the built in communications can be used to raise an alarm if a heart attack is detected. This is managed by an application for Android smartphones that has been developed for this project. The system works for all defined user cases.

Index Terms—Antenna, Planar inverted F-antenna (PIFA), Body area network (BAN), Electrocardiogram (ECG/EKG), Creeping wave, Android, Myocardial infarction.

I. INTRODUCTION

THE most common cause of death in the world is heart disease [1]. Survival rates of heart disease are directly related to the response time of medical personnel [2]. People with myocardial infarction on average do not seek medical care for approximately 1.5 to 2 hours after symptom onset [3]. The vision of this project is to perform a long term and continuous tracking of the electrocardiogram (ECG) of individuals to prevent hazardous or fatal heart related events. The ECG will help detect myocardial infarction, more commonly known as a heart attack, potentially hours before the user would have sought medical treatment.

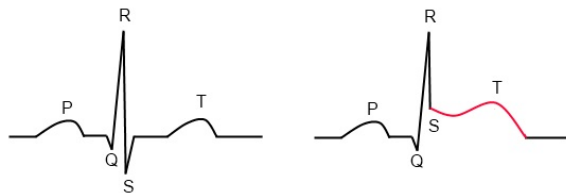


Fig. 1. Normal ECG signal and an ST elevated signal. The relevant sections are the P wave, the QRS complex and the T wave; all marked in the figure. Another important section of the ECG signal for heart disease is the ST segment [4]. The ST segment is the flat, isoelectric section of the ECG between the end of the QRS complex and the beginning of the T wave.

During a myocardial infarction, the ECG readings will have a distinct ST elevation [4]. Fig. 1 shows a normal ECG signal as compared to an ST elevated ECG signal. ST abnormality is one of the most reliable signs of myocardial infarction [4]. When an ST elevation is detected by our device, the user's phone will use its built-in GPS to get the location and instantly alert emergency services. As a significant percentage

of the world's population uses smartphones [5], an Android application was chosen to process the data.

Myocardial infarction is caused primarily by blood clotting. Low doses of the common aspirin pill can act as a blood thinner [6]. The proposed system will be able to notify the user to take an aspirin pill to prevent further blood clotting. The ability to immediately self medicate and the decreased response time will lead to a significant increase of survival rates [7].

There are systems for heart problem management in use today that the proposed system can complement. Some people with a high risk of heart problems have alarms installed in their home that are triggered by pressing a button. The proposed system will have a similar functionality, however it will be automatic and available outside of the home. There are apps available for people with CPR training that will automatically notify if there is an emergency situation in their vicinity [8]. Such features could easily be integrated in the proposed system's Android application.

This report gives an overview of the system and a list of materials with assembly and operation examples. Each part of the system is discussed in more detail. Finally, simulation and testing results are presented and consequently compared and discussed.

II. SYSTEM

An overview of the entire system, called the Gerhards Grabbar (GG) Body Area Network (BAN), can be seen in Fig. 2. The system consists of an ECG sensor that uses electrodes fastened by adhesive tape to the user's chest to measure an ECG signal. The measurements are sent to a microcontroller where they are handled and sent to a Bluetooth transceiver. The data is broadcast to the user's phone via a planar inverted F-antenna (PIFA) that has been designed for this project and has been named the GG Antenna. A smartphone receives the data and processes it in an application called the GG App that displays the ECG and the received signal strength.

A. Materials and Assembly

The components can be seen in Fig. 3 and a bill of materials can be found in Table I. The electrodes are connected to the ECG board via standard electrode cables. The microcontroller is connected by wire to the ECG sensor and attached directly to the transceiver. All components except the antenna and the electrodes are contained in an assembly box.

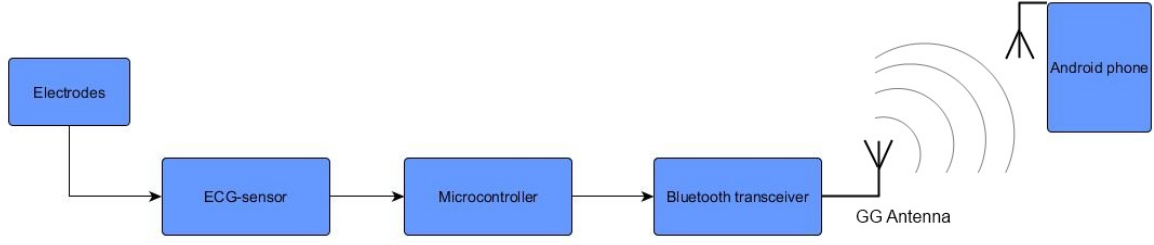


Fig. 2. Block diagram of the GG BAN. Antennas are represented by a standard antenna symbol. Physical connections are represented by arrows while wireless transmission is represented by concentric half-circles.

TABLE I
LIST OF MATERIALS

Description	Name	Retailer	Cost
Electrodes	PlasticsOne Electrode Cable	Electrokit	6.90 USD
ECG sensor	AD8232 Single Lead Heart Rate Monitor	Electrokit	18.64 USD
Microcontroller	Arduino UNO (MEGA 328) rev 3	Electrokit	18.64 USD
Transceiver	Red Bear Lab Bluetooth 4.0 Low Energy Shield v2.1	Electrokit	24.27 USD
Assembly Box	Kemo Electronic Assembly Box	Kjell & Company	5.21 USD
Battery	Kjell & Company	Kjell & Company	2.31 USD
Antenna	GG Antenna	Self made	~ 24 USD
Total cost			100 USD

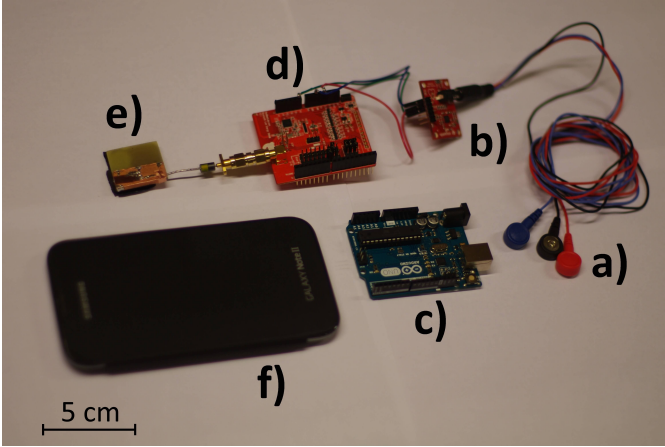


Fig. 3. The components laid out. a) Electrodes b) ECG sensor c) Microcontroller d) Bluetooth transceiver e) GG Antenna f) Android phone.

When using the system, the electrodes are fastened on the user's chest with adhesive tape, the assembly box is placed at a comfortable place on the user's chest and the GG App is downloaded to an Android smartphone and started. Once the sensors are connected, the system is ready to use. The entire system in use is depicted in Fig. 4.

B. Antenna Design

The goal when designing the antenna was to create a small, planar antenna, no larger than $30\text{ mm} \times 30\text{ mm} \times 5\text{ mm}$, with good free space characteristics that would create surface wave propagation along the body it was placed on. To fulfill these specifications, the PIFA design was chosen. A PIFA is a typical small antenna design as it can be designed to be much smaller than the customary $\lambda/2$ size [9]. To enable cheap and quick manufacturing of the prototype antenna, the design was

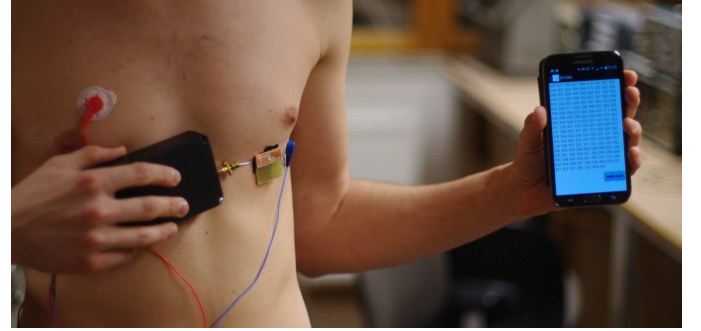


Fig. 4. The entire GG BAN. Two electrodes are placed on the chest and one electrode is placed on the back as a reference. The GG App can be seen printing out measured data.

restricted to concepts realizable by hand and through chemical etching. Thus all vertical metal lines would have to be placed on the sides of the antenna to allow easy application without the use of advanced machinery.

The thickness of the substrate layer was chosen to 3 mm, even though the height of the PIFA increases the bandwidth [10], as room had to be made for the feeding cable attached to the ground plane. This was constructed by gluing two 1.5 mm thick FR-4 laminate plates together. The plates had copper coating which was removed through chemical etching. The feeding structure and the shortening plate was added by using copper tape.

To shield the antenna from the enormous dielectrical load of the body, the ground plane was extended to near the limits of the design specifications, $30\text{ mm} \times 29.6\text{ mm}$. Since the shortening strip had to be placed on the side of the structure, the active element was situated on one side of the square. This had the added benefit of launching the radiation pattern away from the shorted side of the antenna, see Fig. 8, but meant that the antenna could no longer be placed freely.



Fig. 5. The GG Antenna, displaying the ground plane on the left and the active element on the right.

To increase the bandwidth of the antenna, it was fed through a wide plate that distributes the current evenly over the active element [11], [12]. In the ground plane, a feeding plate was inserted to increase reliability of radiation characteristics and ease the manufacturing process. To avoid shortening the antenna through the body, a layer of insulating tape was placed over the exposed feed. The final antenna design can be seen in Fig. 5.

C. Sensor

The sensor solution is composed of three electrodes, two for measurements and one for reference. The electrodes are connected to a board with filters and amplifiers specifically created for ECG signals, called AD8232 Single Lead Heart Rate Monitor.

The signal is processed by a microcontroller, Atmel ATmega328, built into an Arduino UNO. This microcontroller is used because it has enough space to fit the code for controlling the transceiver. The A/D-converter has a 10-bit resolution, which is enough to sample an ECG [13].

The transceiver used is an integrated circuit Bluetooth low energy (BLE) transceiver called nRF8001, that has a maximum power output with a nominal value of 0 dBm. It is connected to the Arduino via a breakout board called Red Bear Lab Bluetooth 4.0 Low Energy Shield v2.1. It communicates with the Arduino using serial peripheral interface (SPI). The transceiver was chosen because it is well documented and has good software libraries. A detailed scheme of the sensor system can be seen in Fig. 6.

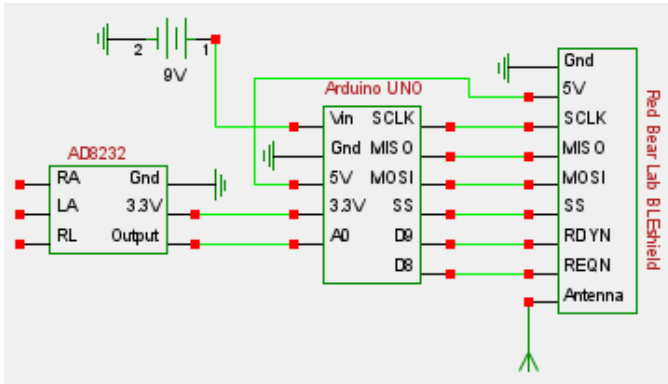


Fig. 6. Scheme of sensor system and the wiring. The three electrodes are connected to the RA, LA, RL inputs on the left side of the AD8232.

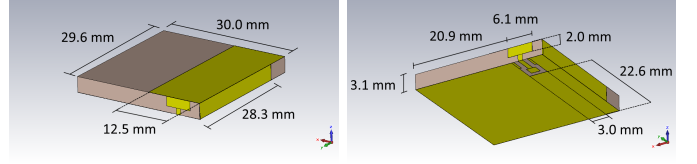


Fig. 7. CST model of the simulated antenna with the measurement specified. The coaxial cable adds 1.9 mm on the height, making the total height 5 mm.

D. Android Application

The Android application called GG App is made to handle data from the sensor. The application has two modes, one where it displays ECG voltage readings and one that shows signal strength, which can be switched between with the press of a button. As it is launched, the application performs a scan for devices and allows the user to select the ECG sensor. The application then receives and interprets data from the sensor and displays it on the screen as a plot. An image of the ECG print-out can be seen in Fig. 10 in Section V.

III. SIMULATIONS & CALCULATIONS

The initial antenna design was simulated in Computer Simulation Technology (CST) Microwave Studio 2014. During the simulation stage of designing the antenna, emphasis was put on creating a resonance that covered the entire Bluetooth band. The antenna was also simulated with a large dielectric block as background to emulate on-body characteristics, $\epsilon_r = 50$ and $\sigma = 1.7 \text{ S/m}$ [14]. Images and measurements of the final antenna design can be seen in Fig. 7. The simulated radiation pattern and return loss can be seen in Fig. 8 & 12, respectively.

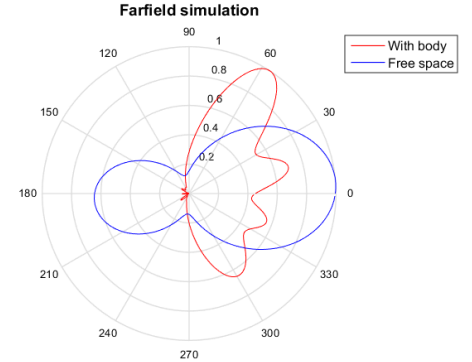


Fig. 8. Normalized farfield radiation pattern from performed simulations, with and without a dielectric block as background material. 0° is the normal direction away from the block. The shorted side of the PIFA faces 270° .

The farfield radiation pattern simulated in Fig. 8 is oriented where the normal direction away from the dielectric block is 0° . When the dielectric block is added, the farfield radiation is pulled down towards its surface. It is also clear that, in the presence of the dielectric block, the antenna becomes noticeably more directional towards 90° , away from the PIFA's shorted side.

TABLE II
LINK BUDGET FOR FREE SPACE TRANSMISSION

Antenna gain	1 dBi
Loss in free space at 1 m	-40 dB
Receiver gain	-5.3 dBi
Total loss	-44.3 dBm

In Fig. 12 seen in Section V, the resonance frequency of the antenna increases as the dielectric load is added. The resonance deepens and thus increases the 10 dB bandwidth of the antenna. This effect arises as the added losses decrease the Q factor of the system and thus increases its bandwidth [15]. The simulated 10 dB bandwidths were 105 MHz and 143 MHz for free space and on-body respectively, thus covering the entire Bluetooth band.

The minimum requirement for Bluetooth receiver sensitivity is -70 dBm [16]. In order to estimate the required free space signal strength, Friis' transmission equation can be employed for given values of received and transmitted gain,

$$\frac{P_r}{P_t} = G_t G_r \left(\frac{\lambda}{4\pi R} \right)^2, \quad (1)$$

where P_r is the power input of the receiving antenna, P_t is the power output of the transmitting antenna, G_t is the antenna gain of the transmitting antenna, G_r is the antenna gain of the receiving antenna, λ is the wavelength and R is the distance between antennas. G_t was simulated to be 1 dBi and G_r was approximated to be -5.3 dBi based on the antenna gain for the LG Nexus 4 [17]. For a distance of 1 m the total loss was estimated to -44.3 dBm, as seen in Table II, indicating that the requirement of received signal strength should be easily met in free space.

When modeling at Bluetooth frequencies, around 2.4 GHz, the electric parameters of the body are approximately $\epsilon_r = 50$ and $\sigma = 1.7 \text{ S/m}$ [14], this results in over 120 dB attenuation for propagation through the body. Thus, it is untenable to consider a solution that sends radiation through the body.

However, as demonstrated in [14], propagation to the other side of the body is still possible, and experimentally proven, without the use of indirect scattering. This is possible through induction of a creeping wave, which propagates along the body's surface. This type of wave also attenuates quickly, but is dependent on polarization [14]. Radiation polarized tangentially to the body's surface will decay at a much greater rate than radiation polarized in the normal direction.

Since the PIFA transmits both vertically and horizontally polarized radiation, it is capable of inducing creeping waves that can propagate longer distances. In [14], the calculation was carried out for a transmitter and receiver on opposite sides of the waist, the resulting attenuation is then about 50-60 dB. For the application of this paper, the considered path stretches from the middle of the torso to the back pocket of the user. Thus, attenuation will be greater due to longer propagation path and irregular geometry. In Table III, there is an approximate link budget for surface waves reaching the back pocket of the user, using the values found in [14]. The transmitting antenna gain was simulated to -1.5 dBi and receiving antenna gain approximated to -5.3 dBi.

TABLE III
LINK BUDGET FOR CREEPING WAVE TRANSMISSION

Antenna gain	-1.5 dBi
Loss on surface	-60 dB
Receiver gain	-5.3 dBi
Total loss	-66.8 dBm

Consequently, the antenna has been chosen considering its ability to generate surface waves. Simulations indicate, as seen in Fig. 8, that the proposed design radiates along the body. The simulated dielectric slab is much smaller than a human torso and has a flat surface due to computational limitations, thus the farfield pattern should be pulled further down in reality. Hence, the GG Antenna should be more than capable of producing the radiation needed for creeping wave propagation.

IV. TESTING

The bandwidth, return loss, efficiency, signal strength and far field radiation of the GG Antenna were measured. The bandwidth and return loss were measured with a vector network analyzer (VNA) in a normal room. The free space efficiency and far field measurements were done in an echo-free Satimo chamber seen in Fig. 9.

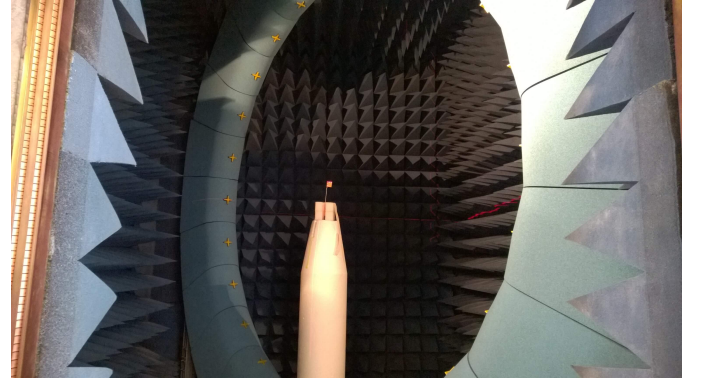


Fig. 9. The SG 24 Satimo measuring chamber at Lite-On Mobile in Lund, Sweden. The GG Antenna is mounted on the test station.

When measuring signal strength of the system in use, the GG App's signal strength measurement function was utilized. The measurements were performed in a normal room with no shielding from interference and at least 2 m of free space between the user and any other object in the room. The signal strength measurements were made with three different test scenarios. The first was signal strength through 1 m of free space. The second was signal strength to the front pocket of the user. The third was signal strength to the back pocket of the user. The ECG voltage readings were plotted in the GG App to see if they properly represent an ECG, the results can be seen in Fig. 10.

V. RESULTS

The ECG in Fig. 10 was measured with the ECG sensor and sent via the GG Antenna to the GG App, where it was plotted as shown. The readings strongly resemble a normal ECG signal, as seen in Fig. 1 in Section I. The noise in the signal is

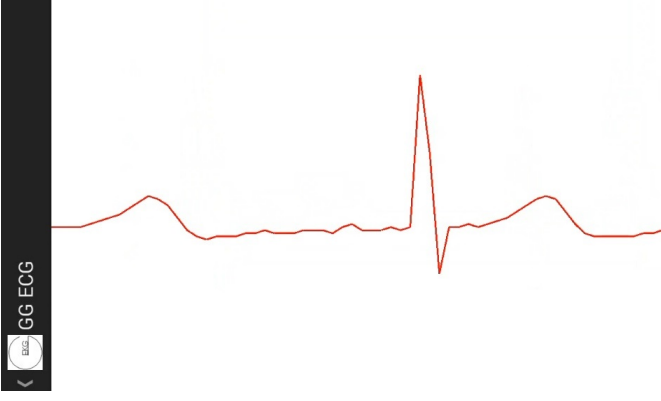


Fig. 10. Screen capture from the GG App of an ECG measured with the GG BAN. The readings strongly resemble a normal ECG signal. The R, S and T segments are all visible and resembling a normal ECG as shown in Fig. 1. The P and Q segments are toned down, but can be suspected in the figure.

heavily dependent on the correct placement of the electrodes on the body. The golden standard for ECG measurement is the 12-lead method [18], using twelve different electrodes to ensure a clear signal. The GG BAN uses only three electrodes to measure a signal, however [18] demonstrates that three electrodes are enough to produce a satisfactory signal. With the use of more electrodes, a more accurate signal could be produced. However, usability has been a priority in designing the GG BAN and thus three electrodes was chosen for simplicity and ease of use.

TABLE IV
SIGNAL STRENGTH MEASURED WITH THE ANDROID APPLICATION

One meter free space	-52 dBm
Front pocket	-55 dBm
Back pocket	-68 dBm

Table IV contains the final measurements for the signal strength received by the GG App. The results are the average value of several measurements. In the estimated link budgets in Table II and III seen in Section III, free space propagation was estimated to -44.3 dBm and creeping wave propagation to -66.8 dBm. The measured results were 7.7 dB and 1.2 dB lower than estimated respectively. There are several factors of uncertainty in the approximations made in the link budgets of Section III. These uncertainties lead to the conclusion that the measured results are close enough to indicate that the system transmits in the expected way.

In the creeping wave estimation, the transmitting and receiving antenna were assumed to be located on either side of the torso. During the back pocket measurement, the transmitting antenna was located at chest height whereas the receiving antenna was situated in the back pocket of the user, thus increasing the travel distance substantially. This increase could account for the lower signal level. However, the received signal is still over the noise floor.

The signal strength in the back pocket is significantly lower than the signal strength in the front pocket. There is little difference in free space distance and there is no possibility of the radiation going through the body, as according to

Section III, that would give a signal approximately 120 dB lower than the free space signal. This leads to the conclusion that the signal reaching the back pocket could in part be of a creeping wave nature. Furthermore, the radiation lobe of the antenna is heavily biased away from its shorted side, see Fig. 8, making creeping wave propagation more likely.

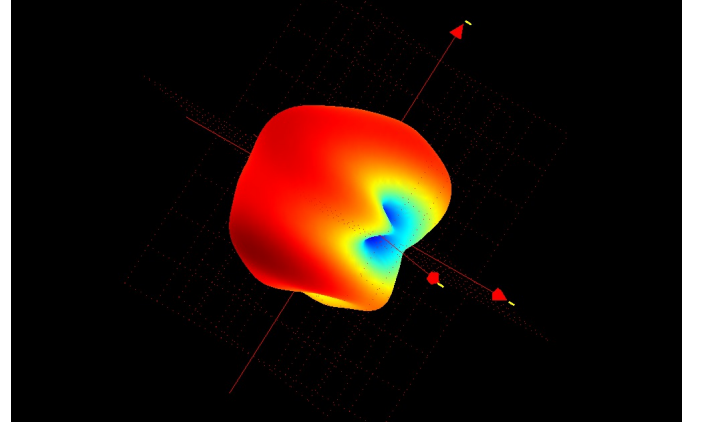


Fig. 11. Farfield free space radiation measurement of the GG Antenna at 2.45 GHz. The measurement was done with the SG 24 Satimo measuring chamber at Lite-On Mobile, Lund. According to the simulations shown in Fig. 8, this 3D pattern will be reduced to a hemisphere when placed on a large dielectric load, such as a body.

The farfield measurement in Fig. 11 is relatively omnidirectional in one hemisphere. This enables the antenna to radiate to various positions on the body. There is, however, a significant minimum located at the grounded side of the active element. When the system is fastened to the user's body, the antenna is oriented in such a way as to point this minimum towards the user's head. Fig. 8 shows that the addition of a body bends the farfield radiation pattern towards the user. Thus, the farfield measurement seen in Fig. 11 is likely to do the same once the antenna is placed on the body.

The design specifications indicate that prioritized receiving locations are areas used for phone storage, such as pockets or somewhere in the user's vicinity. The pattern in Fig. 11 indicates that the antenna might have trouble transmitting to the phone when it is actively used in a phone call or other similar applications. However, since the system is located on the user's chest, the transmitting distance to the phone during a call will be relatively short and thus not create an issue.

In Fig. 12, the measured and simulated return loss for free space and on-body transmission is plotted. Interestingly, the measured resonances are deeper than the simulated ones. The same behaviour is observed in measurements and simulations; when the antenna is placed on the body, the resonance frequency increases slightly and deepens. The effect of the body is not as drastic during measurement as it is for simulations.

The efficiency in Fig. 13 is relatively even over the Bluetooth band, this implies that the radiation characteristics of the antenna are stable. Since the efficiency is above -2.5 dBi, the antenna works for the desired frequencies. As expected, the measured efficiency is lower than the simulated one of -1 dBi, but still acceptable.

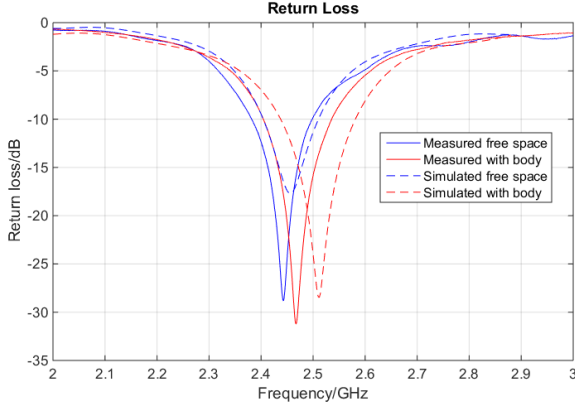


Fig. 12. Simulated and measured return loss of the GG Antenna. During simulation, the body was modelled as a dielectric slab of dimensions $30\text{ mm} \times 400\text{ mm} \times 400\text{ mm}$. The simulated 10 dB bandwidths were 105 MHz, 4.3 %, and 143 MHz, 5.7 %, for free space and on-body, respectively. The measured 10 dB bandwidths were 116 MHz, 4.7 %, and 132 MHz, 5.4 %, for free space and on-body, respectively.

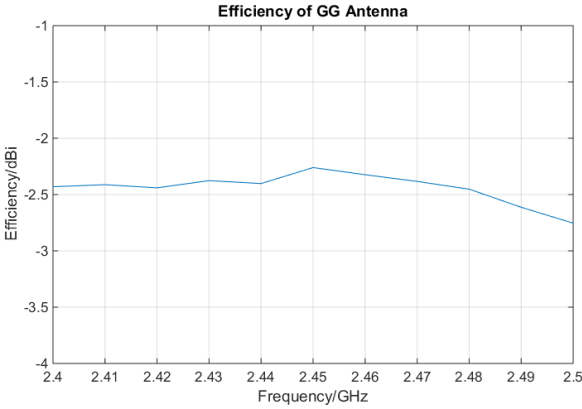


Fig. 13. Measured efficiency for the GG Antenna. The efficiency is relatively even. The simulated efficiency was -1 dBi.

VI. CONCLUSIONS

This paper demonstrates that the transmission of Bluetooth signals in a BAN is possible with a simple antenna design. Through the use of creeping wave propagation, the signal can be made to reach locations on the body that are inaccessible without scattering off nearby objects. It has been experimentally shown in this paper that this mode of transmission meets the minimum requirement for Bluetooth signals. Thus, any Bluetooth device should be able to maintain contact with the GG BAN.

The components used in this prototype are relatively cheap and not tailored for measuring ECG signals. Higher quality hardware and more electrodes would give a clearer and more reliable signal. However, the system presented here has put an emphasis on cheap manufacturing and easy of use.

In Fig. 10 it was shown that a smartphone's signal processing is enough to measure a recognisable ECG curve. As a large percentage of people today own a smartphone or a similar device, it ensures that the GG BAN can be distributed easily. The cost of the entire system is relatively low, and by utilizing integrated circuits and a microcontroller tailored for

this particular application, the prototype can be made even smaller and more energy efficient. Thus, the system can be mass produced at a low cost, and sold separately for a low price to patients or hospitals.

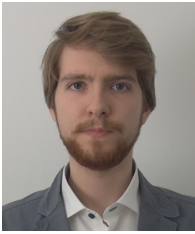
Reliability of correct ECG signals is still an issue for this type of an application. However, this paper has demonstrated that it is possible to wirelessly transmit such a signal to commonly available devices. This is a step in the right direction for full time monitoring of high risk patients in the future. As the signal received in Fig. 10 is relatively noise-free and shows a clear ST-segment, it is possible to detect an ST-elevation with further software development, thereby being able to predict heart attacks.

ACKNOWLEDGMENT

A big thank you to our advisors and supervisors Anders Sunesson and Jakob Helander, without whom we would not have completed this paper. Our thanks extend to Lite-On Mobile, for generously letting us use their Satimo chamber. We would also like to thank Christian Antfolk for meaningful advice, Martin Nilsson for help with etching and Andreas Johansson for his soldering expertise. Additionally, we would like to thank Bertil Bengtsson and Gerhard Kristensson.

REFERENCES

- [1] *The Top 10 Causes of Death*. World Health Organization, 2014.
- [2] J. P. Pell, J. M. Sirel, et al. Effect of reducing ambulance response times on deaths from out of hospital cardiac arrest: cohort study. *BMJ*, 322(7299):1385–1388, Jun. 2001.
- [3] P. T. O'Gara, F. G. Kushner, et al. 2013 accf/aha guideline for the management of st-elevation myocardial infarction: A report of the american college of cardiology foundation/american heart association task force on practice guidelines. *Circulation*, 127(4):e362–e425, Dec. 2013.
- [4] E. Burns. *The ST Segment*. Life in the Fast Lane, 2013.
- [5] *2 Billion Consumers Worldwide to Get Smart(phones) by 2016*. eMarketer, Dec. 2014.
- [6] Anti-clotting agents explained. *Stroke Connection Magazine*, Jul./Aug. 2003.
- [7] B. Gulli. *Emergency Care and Transportation of the Sick and Injured*. Jones & Bartlett Publishing, 2009.
- [8] Pulsepoint. <http://www.pulsepoint.org/>, 2015.
- [9] K. Wong. *Planar Antennas for Wireless Communications*. Wiley-Interscience, 2003.
- [10] L. C. Godara. *Handbook of Antennas in Wireless Communications*, volume 4. CRC press, 2014.
- [11] R. Feick, H. Carrasco, et al. Pifa input bandwidth enhancement by changing feed plate silhouette. *IEEE Electronics Lett.*, 40(15):921–922, Jul. 2004.
- [12] H.T. Chattha, Yi Huang, and Yang Lu. Pifa bandwidth enhancement by changing the widths of feed and shorting plates. *IEEE Antennas Wireless Propag. Lett.*, 8:637–640, Jul. 2009.
- [13] M. Raju. *Heart-Rate and EKG Monitor Using the MSP430FG439*. Texas Instruments, 2007.
- [14] T. Alves, B. Poussot, et al. Analytical propagation modeling of ban channels based on the creeping-wave theory. *IEEE Trans. Antennas Propag.*, 59(4):1269 – 1274, Apr. 2011.
- [15] R.E. Collin and S. Rothschild. Evaluation of antenna q. *IEEE Trans. Antennas Propag.*, 12(1):23–27, Jan. 1964.
- [16] *Bluetooth® Core Specification 4.2*. Bluetooth, 2014.
- [17] J.Tsai. *FCC RF Test Report FR291007A*. FCC, Sep. 2012.
- [18] R. Antonicelli, C. Ripa, et al. Validation of the 3-lead tele-ecg versus the 12-lead tele-ecg and the conventional 12-lead ecg method in older people. *Journal of Telemedicine and Telecare*, 18(2):104–108, Jan. 2012.



Georg Wolgast is a Master of Science in Engineering, Engineering Physics and Engineering Nanoscience undergraduate student, currently studying his third year at the Faculty of Engineering, Lund University.



Casimir Ehrenborg received his M.Sc. in engineering physics from Lund university in 2014. He is currently a Ph.D. student at the Electromagnetic Theory Group, Department of Electrical and Information Technology at Lund university. His research interests include stored energy expressions, radiation center, Q-factors and physical bounds.



Alexander Israelsson is a Master of Science in Engineering, Engineering Physics undergraduate student, currently studying his third year at the Faculty of Engineering, Lund University.



Edvard Johansson is a Master of Science in Engineering, Engineering Physics undergraduate student, currently studying his third year at the Faculty of Engineering, Lund University.



Hampus Månefjord is a Master of Science in Engineering, Engineering Physics undergraduate student, currently studying his third year at the Faculty of Engineering, Lund University.